Inorganic Chemistry

Article

pubs.acs.org/IC

Polarized Micropores in a Novel 3D Metal–Organic Framework for Selective Adsorption Properties

Chengli Jiao,[†,‡] Jian Zhang,[†] Shuang Wang,[†,‡] Xiaoliang Si,[†,‡] Wansheng You,[§] Zhangpeng Li,[∥] Zhonggang Wang,[⊥] Hao Yu,[⊥] Zelimir Gabelica,[#] Huai-Ying Zhou,[&] Lixian Sun,*[,†,&] and Fen Xu*[,¶]

[†]Materials and Thermochemistry Laboratory, Dalian Institute of Chemical Physics, Chinese Academy of Sciences, 457 Zhongshan Road, Dalian 116023, People's Republic of China

[‡]Graduate School of the Chinese Academy of Sciences, Beijing 100049, People's Republic of China

[§]Institute of Chemistry for Functionalized Materials, Liaoning Normal University, Dalian 116029, People's Republic of China

[∥]State Key Laboratory of Solid Lubrication, Lanzhou Institute of Chemical Physics, Chinese Academy of Sciences, Lanzhou 730000, People's Republic of China

[⊥]Department of Polymer Science and Engineering, Dalian University of Technology, Dalian, 116012, People's Republic of China

[#]LPI-GSEC, ENSCMu, Université de Haute Alsace, F-68093 Mulhouse, France

[¶]College of Chemistry and Chemical Engineering, Liaoning Normal University, Dalian 116029, People's Republic of China

[&]Department of Materials Science and Engineering, Guilin University of Electronic Technology, Guilin 541004, People's Republic of China

Supporting Information

ABSTRACT: A novel 3D porous metal–organic framework with 1D polarized channels was synthesized, and its adsorption properties for gas separation and chemical sensing were studied. The framework shows a preferential adsorption of CO_2 over N_2 with a selectivity of 22:1. It also exhibits a very good sensitivity to water with respect to most of the organic solvents in view of chemical sensing applications.

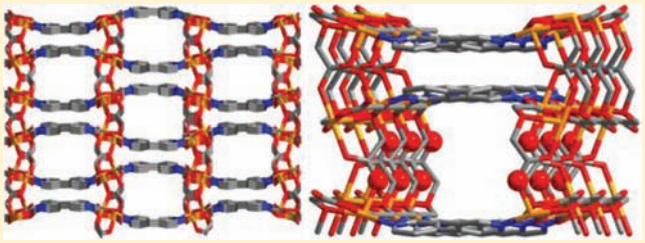

INTRODUCTION

Metal–organic frameworks (MOFs) have recently received significant attention as functional materials because of their various potential applications in catalysis, gas storage, chemical separations, sensing, ion exchange, drug delivery, and optics.[1] Because of their large surface areas, adjustable pore sizes, and controllable functionalities, MOFs are widely explored as promising candidates for adsorptive separations and purification purposes. Recently, several MOFs with large adsorption capacities and high selectivity for a number of small molecules (CO_2, H_2, CH_4, alkanes, and alkenes) have been reported.[2] In particular, for separation of CO_2/CH_4 and CO_2/N_2, great efforts have been made to tune pore sizes and surface chemistry of MOFs.[3] Taking into account the inherent polarity or polarizability of guest molecules, tuning the pore nature with a rational design strategy is an effective method.[4]

Aromatic carboxylic acids are widely used as rigid linkers in the construction of porous networks of MOFs.[5] Another important group of MOFs can be constructed based on flexible ligands. Oxydiacetic acid is a flexible multidentate ligand with five potential oxygen-donor atoms (four from two carboxylate groups and one from the ether function), which can coordinate to one or more metal centers in different ways. Both oxydiacetic acid (H_2oda) and its sulfur analogue thiodiacetic acid (H_2tda) have been widely explored as multitopic linkers for synthesizing coordination polymers with interesting magnetic properties.[6]

Here we report the synthesis of a novel 3D microporous metal–organic framework, Co_2(oda)$_2$(4,4′-bipy)·DMF, with 1D channels of two different sizes. Upon running the sorption isotherms of N_2, H_2, CO_2, and CH_4, it was noticed that Co_2(oda)$_2$(4,4′-bipy) had a potential capability for CO_2/N_2 separation with a high selectivity of 22:1. On the other hand, adsorption and desorption of a series of small solvent molecules with variable polarities conducted using the in situ quartz crystal microbalance (QCM) technique indicated that Co_2(oda)$_2$(4,4′-bipy) had a fairly good sensitivity for water.

EXPERIMENTAL SECTION

General Procedures. All reagents and chemicals were available commercially and of analytical grade without further purification prior to use, unless specifically stated elsewhere. Powder X-ray diffraction patterns were collected on an X'Pert PRO X-ray diffractometer operating at 40 kV and 40 mA with Cu Kα radiation (λ = 1.5418 nm). Thermogravimetric analysis (TGA) was carried out on a Cahn Thermax 500 instrument with a heating rate of 10 °C/min under flowing air. The sorption isotherms for CO_2, N_2, H_2, and CH_4 were

Received: November 13, 2011
Published: April 13, 2012

   dx.doi.org/10.1021/ic202769e | Inorg. Chem. 2012, 51, 5022–5025

measured using a Micrometrics ASAP 2010 (Quantachrome) device. An activated sample of 100.0–200.0 mg was used for sorption measurements, maintained at 77 K with liquid nitrogen and at 273 K using a water–ice bath. The activated sample was outgassed at 150 °C for 6 h using a high-vacuum line prior to gas adsorption. Adsorption properties of H_2O, CH_3OH, and other small solvent molecules were characterized on a quartz crystal microbalance (Maxtek, USA).

Quartz Crystal Microbalance Test. The piezoelectric sensing strategy developed on a quartz crystal microbalance is based on a very high mass sensitivity. A decrease of the QCM frequency is directly proportional to the increase of the film mass. Prior to each test, traces of water in organic solvents were removed using anhydrous $MgSO_4$. The QCM disk was treated with a piranha solution for 10 min, rinsed with deionized water, and dried in air. A 6 mg amount of **1** was dispersed in an ultrasound-assisted 6 mL DMF solution for 30 min. A first 15 μL solution was deposited on the 1.13 cm^2 chromium/platinum film on 9 MHz AT-cut crystals (Maxtek Inc.) and dried in air. An initial frequency was recorded. The sensing measurements with coated quartz crystals were conducted in a sealed chamber (0.5 L) at room temperature, the chamber being evacuated to below 0.01 MPa before each solvent dose was injected. When a stable resonant frequency was obtained, the chamber had to be evacuated so as to monitor the desorption of the solvent molecules and guarantee a total desorption until the frequency recovered to its initial value.

Synthesis of $Co_2(oda)_2(4,4'\text{-bipy})\cdot DMF$ (1·DMF). A mixture of $Co(NO_3)_2\cdot 6H_2O$ (0.29 g, 1 mmol), oxydiacetic acid (0.13 g, 1 mmol), 4,4′-bipyridine (0.16 g, 1 mmol), and DMF (10 mL) was sealed in a 40 mL Teflon-lined stainless steel autoclave and heated at 120 °C for 48 h, then left to cool naturally to room temperature. Red, blocky crystals suitable for X-ray analysis were filtered, washed with DMF, and dried at 50 °C under vacuum overnight. Yield: 0.241 g or 78% based on Co^{II}. CCDC 841684. Anal. Calcd for **1**·DMF: C, 41.26; H, 3.79; N, 6.87. Found: C, 42.50; H, 4.46; N, 6.43.

RESULTS AND DISCUSSION

The crystal structure of $Co_2(oda)_2(4,4'\text{-bipy})\cdot DMF$ (**1**·DMF) with a 3D framework is shown in Figure 1. Each Co^{II} center adopts pseudo-octahedral symmetry upon coordinating three oxygen atoms from a chelate oxydiacetate group (O1, O2, and O5), two carboxylate oxygens (O3 and O4) from other oxydiacetate groups, and one N atom from the 4,4′-bipyridine ligand that is bridging two cobalt centers (Figure 1a). The Co(oda) fragment adopts a folded (fac) conformation rather than a planar (mer) conformation, the former being only occasionally observed in M(oda) complexes.[6a] In turn, each oda ligand bridges three Co^{II} centers, while each 4,4′-bipyridine ligand bridges two Co nodes, leading to an overall 3D framework containing 1D channels with window sizes of 3.7 × 11.2 and 8.6 × 6.7 $Å^2$ running along the *c* axis, filled with DMF solvent molecules (Figure 1b–d). Powder X-ray diffraction patterns for **1**·DMF are shown in Figure S1. The diffraction peaks of the as-synthesized MOF match well the simulated pattern on the basis of the single-crystal structure, which indicates that **1**·DMF is the major product.

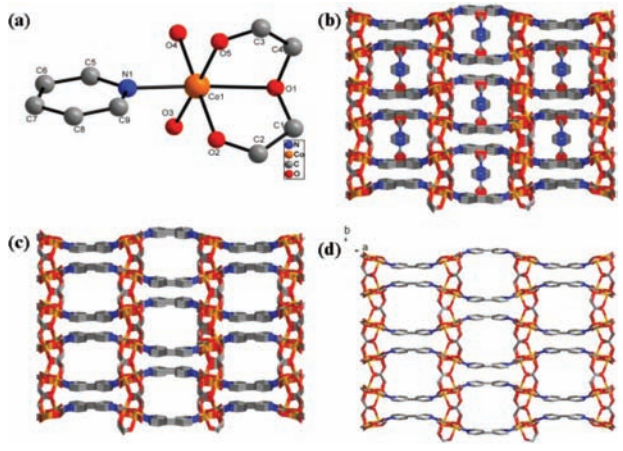

Figure 1. Structure of the crystal **1**·DMF: (a) the asymmetric unit and Co^{II} coordination environment; (b) view of the 3D framework with DMF solvent molecules entrapped in the channels; (c) view of the 3D framework with DMF solvent molecules omitted; (d) view of the 3D framework seen on the *ab* plane with DMF solvent molecules omitted.

The overall thermal stability of **1**·DMF and its temperature of desolvation were evaluated by thermogravimetric analysis. The TGA curve (Figure S2) shows a two-step weight loss in the 30–700 °C temperature range. The first loss starts at 116 °C and reaches about 10.55% at 200 °C, corresponding to the release of one DMF solvent molecule per formula unit (calcd 11.96%). The as-synthesized framework was further activated at 210 °C for 4 h so as to yield a fully desolvated framework for sorption and separation uses. The total DMF loss was confirmed by TGA and PXRD (Figures S3 and S4, respectively). The PXRD pattern of the activated MOF (**1**) is almost the same as that of the as-synthesized MOF (**1**·DMF), indicating that the framework retains its structural integrity once the guest molecules are removed.

Considering that the dimension of the channels can give access to only small guest molecules, H_2 (2.89 Å), CO_2 (3.3 Å), O_2 (3.46 Å), N_2 (3.64 Å), and CH_4 (3.8 Å) were selected as probes to study the gas sorption and separation properties of compound **1**.

To our surprise, **1** does not adsorb N_2 and H_2 gases even at 77 K (Figure 2). However, it adsorbs CO_2 and CH_4 gases to show type I isotherms at 273 K, which is characteristic of microporous materials. The adsorption and desorption branches for CO_2 and CH_4 show a slight hysteresis attributed to the presence of intercrystalline voids. **1** adsorbs CO_2 up to 28.02 $cm^3\ g^{-1}$ (1.3 mmol g^{-1}, 5.7 wt % at STP) at 273 K and 1 bar. At 273 K, **1** exhibited a preferential adsorption of CO_2 over N_2 with a selectivity of 22:1, calculated from the ratios of initial slopes of the CO_2 and N_2 adsorption isotherms (Figure S5).[2a]

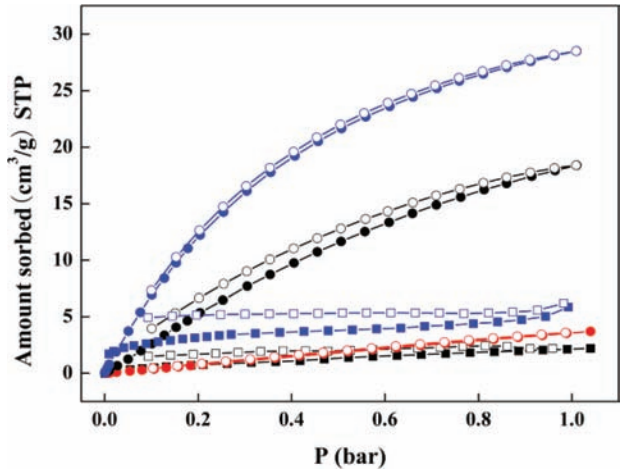

Figure 2. Gas sorption isotherms of **1** at various temperatures. Solid and open symbols represent adsorption and desorption, respectively: H_2 (square, black) and N_2 (square, blue) at 77 K; N_2 (circle, red), CH_4 (circle, black), and CO_2 (circle, blue) at 273 K.

dx.doi.org/10.1021/ic202769e | Inorg. Chem. 2012, 51, 5022–5025

In the framework structure, atoms O3 of oxydiacetate groups are alternately exposed inside the relatively big 1D channels (Figure 3), so that the channels of **1** are globally polarized.

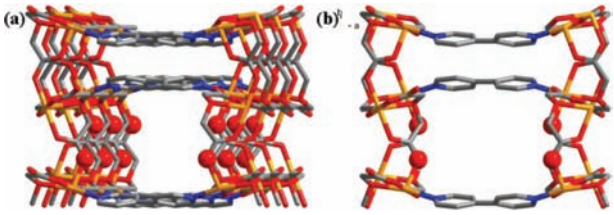

Figure 3. Detailed structure of the **1** framework system: (a) O3 atoms alternately protruding within the channels (red balls); (b) view along [001].

In Figure 2, CO_2 is the most strongly adsorbed molecule, probably due to its significant quadrupole moment (-13.7×10^{-40} C·m^2) inducing a stronger interaction with the framework.[7] Indeed a remarkable CO_2 uptake observed on aluminum naphthalenedicarboxylate MOF, Al(OH)(1,4-ndc)·2H_2O, was also explained by favorable interactions of CO_2 with the π-electron clouds present near the polar OH groups protruding toward the host channels.[8] In our case, one can, for example, imagine that the polarized δ^- charged oxygens induce an electric field in the channels. The polarizable CO_2 molecule that is approaching this negatively charged center is therefore also polarized as $O^{\delta-}-C-O^{\delta+}$ by these electron clouds. The mutual interaction between the $-O^{\delta+}$ end of CO_2 and the framework $-O^{\delta-}$ is simply induced by the electric field gradient that is created in such systems. The field is the strongest next to the charged framework oxygens where the interaction occurs and sharply decreases with the distance inside the polarized micropore. CH_4 shows stronger adsorption than N_2, which has been observed and reported previously.[2c,9] This is attributed to the higher polarizability of CH_4 (26.0×10^{-25} cm^3) vs N_2 (17.7×10^{-25} cm^3),[7] inducing an attraction to the host framewok.

Because of the polar channel interior, small solvent molecules such as methanol, water, acetone, pyridine, and chloroform were tested to study the chemical sensing of framework **1**, using the quartz crystal microbalance. The kinetic diameters for methanol, water, acetone, pyridine, and chloroform are 3.9, 2.7, 4.6, 4.6, and 5.4 Å, respectively.[10] A preferred interaction between polar solvent molecules such as water (and, to a lesser extent, methanol) and the internal δ^- polarized oxygens is likely to occur. As expected, the sensor showed no response to acetone, pyridine, and chloroform, which exhibit a low polarity.

Figure 4a shows frequency changes for a **1**-coated QCM, with the injection of methanol varying from 10 to 80 μL in a 0.5 L chamber. The frequency shift undergoes a small change with the increase in the methanol content. The **1**-coated QCM was exposed to different injections of water (from 1 to 10 μL) in the same chamber, and the corresponding frequency shift is shown in Figure 4b. A much higher frequency shift is obtained, indicating that the **1**-coated QCM shows a significantly higher sensitivity to water than methanol. It is worth noting that the desorption of water is rather hard for the long desorption time, although the adsorption/desorption process of water is totally reversible. These differences were attributed to the larger polarity of water than of methanol, responsible for the strong interaction of water with the host framework. The adsorption mechanism probably involves a classical interaction between a

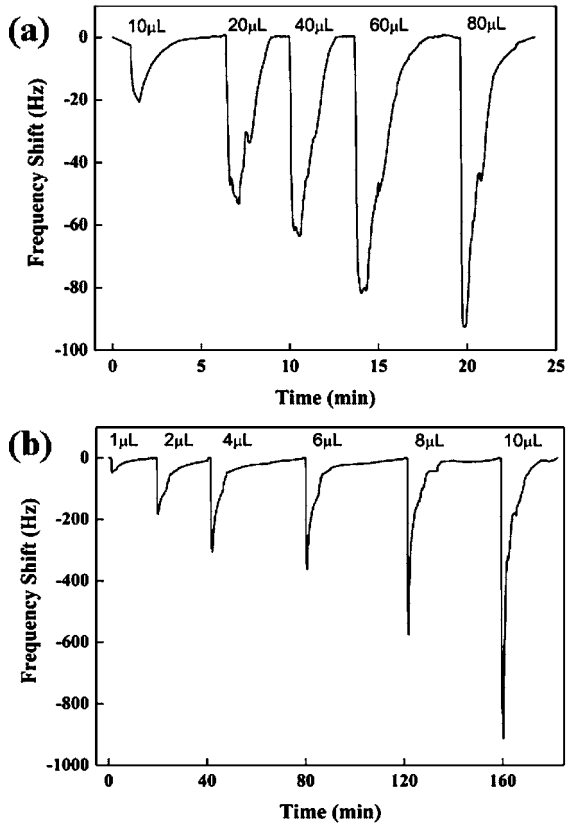

Figure 4. Frequency shift for **1**-coated QCM response to (a) methanol and (b) water. (a) The injected volumes of 10, 20, 40, 60, and 80 μL correspond to methanol concentrations in the chamber of respectively 16, 32, 64, 96, and 128 ppm. (b) The injected volumes of 1, 2, 4, 6, 8, and 10 μL, correspond to water concentrations in the chamber of respectively 2, 4, 8, 12, 16, and 20 ppm.

polar molecule (water with delocalized charges) and the δ^- polarized oxygens in the channels, either through some dipole–dipole interactions or through hydrogen bonding, which is stronger. Straigtforward potential applications of the **1** framework structure with polarized micropores include water monitoring, gas drying, or removal of water from water–methanol (or other solvent) mixtures.

CONCLUSIONS

In conclusion, we have successfully synthesized a novel 3D porous metal–organic framework, $Co_2(oda)_2(4,4'\text{-bipy})\cdot$DMF, characterized by 1D polarized channels with two different sizes. The framework without DMF exhibits selective sorption properties for CO_2 over N_2 with a selectivity ratio of 22:1, partly due to the quadrupolar moment of CO_2, which favors a rather strong interaction with the polarized micropores. As a result of different polarities of small solvent molecules, the framework shows a higher sensitivity toward water over organic solvents. Further research on the construction of pore- and surface-controllable MOFs for guest separation and sensing is in progress.

ASSOCIATED CONTENT

Supporting Information

CIF of **1**·DMF, crystallography of **1**·DMF, TGA plots, XRD patterns, and slope calculation for CO_2/N_2 at 273 K. This

dx.doi.org/10.1021/ic202769e | Inorg. Chem. 2012, 51, 5022–5025

material is available free of charge via the Internet at http://pubs.acs.org.

AUTHOR INFORMATION

Corresponding Author

*E-mail: lxsun@dicp.ac.cn; fenxu@lnnu.edu.cn. Fax: (+86)-411-84379213.

Notes

The authors declare no competing financial interest.

ACKNOWLEDGMENTS

This work was financially supported by the "973 Project" (2010CB631303), NSFC (20833009, 51071146, 21173111, 20903095, 51071081, 51101145, U0734005, and 51102230), Liaoning BaiQianWan Talents Program (No. 2010921050), Liaoning Education Committee (L2010223), Solar Energy Action Plan of CAS, IUPAC (Project No. 2008-006-3-100), The Joint Project of Guangdong Province and Chinese Academy of Sciences (2010A090100034), and the State Key Laboratory of Explosion Science and Technology, Beijing Institute of Technology (Grant No. KFJJ10-1Z).

REFERENCES

(1) (a) Banerjee, D.; Kim, S. J.; Wu, H. H.; Xu, W. Q.; Borkowski, L. A.; Li, J.; Parise, J. B. *Inorg. Chem.* **2011**, *50*, 208−212. (b) Miller, S. R.; Heurtaux, D.; Baati, T.; Horcajada, P.; Greneche, J. M.; Serre, C. *Chem. Commun.* **2010**, *46*, 4526−4528. (c) Chen, B. L.; Wang, L. B.; Xiao, Y. Q.; Fronczek, F. R.; Xue, M.; Cui, Y. J.; Qian, G. D. *Angew. Chem., Int. Ed.* **2009**, *48*, 500−503. (d) Nouar, F.; Eckert, J.; Eubank, J. F.; Forster, P.; Eddaoudi, M. *J. Am. Chem. Soc.* **2009**, *131*, 2864−2870. (e) Yoon, J. W.; Jhung, S. H.; Hwang, Y. K.; Humphrey, S. M.; Wood, P. T.; Chang, J. S. *Adv. Mater.* **2007**, *19*, 1830−1834. (f) Rosi, N. L.; Eckert, J.; Eddaoudi, M.; Vodak, D. T.; Kim, J.; O'Keeffe, M.; Yaghi, O. M. *Science* **2003**, *300*, 1127−1129.

(2) (a) An, J.; Geib, S. J.; Rosi, N. L. *J. Am. Chem. Soc.* **2010**, *132*, 38−39. (b) Seo, J.; Jin, N.; Chun, H. *Inorg. Chem.* **2010**, *49*, 10833−10839. (c) Bae, Y. S.; Farha, O. K.; Hupp, J. T.; Snurr, R. Q. *J. Mater. Chem.* **2009**, *19*, 2131−2134.

(3) (a) Zheng, B. S.; Bai, J. F.; Duan, J. G.; Wojtas, L.; Zaworotko, M. J. *J. Am. Chem. Soc.* **2011**, *133*, 748−751. (b) Chen, Y. F.; Lee, J. Y.; Babarao, R.; Li, J.; Jiang, J. W. *J. Phys. Chem. C* **2010**, *114*, 6602−6609.

(4) Henke, S.; Schmid, R.; Grunwaldt, J. D.; Fischer, R. A. *Chem.−Eur. J.* **2010**, *16*, 14296−14306.

(5) (a) Deng, H.; Doonan, C. J.; Furukawa, H.; Ferreira, R. B.; Towne, J.; Knobler, C. B.; Wang, B.; Yaghi, O. M. *Science* **2010**, *327*, 846. (b) Chun, H.; Jung, H. *Inorg. Chem.* **2009**, *48*, 417−419.

(6) (a) Grirrane, A.; Pastor, A.; Alvarez, E.; Mealli, C.; Ienco, A.; Rosa, P.; Galindo, A. *Eur. J. Inorg. Chem.* **2007**, 3543−3552. (b) Wang, Y.; Cheng, P.; Chen, J.; Liao, D. Z.; Yan, S. P. *Inorg. Chem.* **2007**, 4530−4534. (c) Grirrane, A.; Pastor, A.; Alvarez, E.; Mealli, C.; Ienco, A.; Masi, D.; Galindo, A. *Inorg. Chem. Commun.* **2005**, *8*, 463−466.

(7) (a) Rallapalli, P.; Prasanth, K. P.; Patil, D.; Somani, R. S.; Jasra, R. V.; Bajaj, H. C. *J. Porous Mater.* **2011**, *18*, 205−210. (b) Peck, E. R.; Khanna, B. N. *JOSA* **1966**, *56*, 1059−1063. (c) Buckingham, A. D. *Q. Rev. Chem. Soc.* **1959**, *13*, 183−214. (d) Cuthbertson, C.; Cuthbertson, M. *Proc. R. Soc. A* **1920**, *97*, 152−159. (e) Howell, J. T. *Phys. Rev.* **1915**, *6*, 81−93.

(8) Comotti, A.; Bracco, S.; Sozzani, P.; Horike, S.; Matsuda, R.; Chen, J.; Takata, M.; Kubota, Y.; Kitagawa, S. *J. Am. Chem. Soc.* **2008**, *130*, 13664−13672.

(9) (a) Bae, Y. S.; Spokoyny, A. M.; Farha, O. K.; Snurr, R. Q.; Hupp, J. T.; Mirkin, C. A. *Chem. Commun.* **2010**, *46*, 3478−3480. (b) Harlick, P. J. E.; Tezel, F. H. *Sep. Purif. Technol.* **2003**, *33*, 199−210.

(10) (a) McCool, B. A.; DeSisto, W. J. *Ind. Eng. Chem. Res.* **2004**, *43*, 2478−2484. (b) Eddaoudi, M.; Li, H.; Yaghi, O. M. *J. Am. Chem. Soc.* **2000**, *122*, 1391−1397. (c) Gales, L.; Mendes, A.; Costa, C. *Carbon* **2000**, *38*, 1083−1088. (d) Breck, D. W. *Zeolite Molecular Sieves*; John Wiley & Sons: NewYork, 1974.